

A study on deflections of GFRP reinforced concrete beams.

Enio Deneko

Polytechnic University of Tirana, Faculty of Civil Engineering, Tirana, Albania
enioudeneko@hotmail.com

Abstract: Steel reinforcing bars have not performed well in applications where members were subject to corrosive environments. Alkaline concrete protection can provide relatively good protection of the steel reinforcement, but when these are exposed to an aggressive environment or the protection breaks down, the reinforcement starts the corrosive process and it leads to rupture and fragmentation of the protective layer of concrete.

These reasons lead to high maintenance costs, repairing or even replacing them. This problem prompted a lot of researchers to seek alternative materials with characteristics better than steel to be used in construction. GFRP bars, which are fibers with high resistance immersed in a polymer resin matrix, with a high tensile resistance and also resistant to corrosion, emerged in the 1990s as an alternative to replace steel rods. The use of GFRP is increasingly accepted by the countries, which are trying to create or adopt special codes for their use in building structures.

This paper will take a quick look over GFRP materials and their mechanical properties, but also will aim to provide some ideas on the study of concrete members reinforced with GFRP bars and their design based on SLS method as it represents the most problematic one, focusing on deflections of GFRP reinforced beams.

Keywords: GFRP, CONCRETE, SLS DESIGN, DEFLECTION, CURVATURE, MOMENT OF INERTIA.

1. Introduction

This study aims at an investigation on the new trend of using GFRP bars as internal reinforcement in concrete members. It intends to:

- Identify some of GFRP's mechanical properties, as a possible material to be used as internal reinforcement in concrete members.

- Investigate, using theoretical methods and application, through literature and codes, the flexural behavior of concrete members reinforced with GFRP bars and their design based on Service Limit States (SLS), in terms of cracks width, deformations and deflections under service and sustained loads.

Through experimental tests carried out on beams reinforced with GFRP bars, will be studied their failure modes, deflections, and cracking, and the comparison of experimental data with theoretical values based on existing codes.



Fig. 1 GFRP reinforcing bars used in a concrete slab

2. Methodology

Glass fibers (GFRP) are used as reinforcing bars as internal reinforcement, as external reinforcing sheets and structural profiles produced with pultrusion. They are sensitive to moisture, to the presence of salts and alkali and suffer the effect of cracks, resistance loss, and rupture under constant loading. They are good electrical and thermal insulation and with low cost of reinforcing fibers.

Glass fibers (GFRP), are among the most common of FRP bars and they are offered by a large number of manufacturers in the world. GFRP bars are produced in size ranging from 3/8 to 1 3/8 in. (9 – 41 mm), no.3 to no.13 bars, but ASLAN 100 produces FRP bars starting from No. 2 (6 mm) to No. 13 (41 mm).

Because the FRP mechanical properties differ from those of steel, particularly the module of elasticity that is significantly lower in FRP bars than in steel bars, the elastic behavior up to fracture, lack of ductility, etc., the SLS design, especially the cracking and deflection criterion may control the design of GFRP-RC beams. SLS design of GFRP-RC beams takes into account these major problems:

- Cracking
- Deformation and deflection
- Stresses in the material

The most problematic ones are the first two problems, as these guarantee the functionality of the structure throughout its lifetime.

The service conditions also depend on the importance of the structure and the environment. The problem that appears is similar to the already known one of concrete structures reinforced with steel bars. Because GFRP bars have a much lower modulus of elasticity than steel bars, the serviceability limit state dictates the design of concrete sections reinforced with GFRP bars. Permissible deflections for service loads in these structures are taken the same as for all other structures, so the relevant design conditions must be applied. The permitted crack widths for these elements are not the same as for conventional concrete elements reinforced with steel bars, due to the greater corrosion resistance of GFRP bars.

The methods, the models, and the restrictions used during the analysis must be different; in addition, a large number of existing materials in the field of FRP bars production, with quite different mechanical characteristics and not as unified as for steel bars, requires special ways to solve these problems.

Only some countries have implemented specific design codes:

- American Code (ACI-440R-96),
- Canadian Code (ISIS CANADA/CSA S806-02)
- Norwegian Code (EUROCRETE)
- Italian Code (CNR-DT203/2006)
- Japanese Code (JSCE)

3. Deflections of GFRP-RC beams under service loads

Similar to the case of steel-reinforced concrete members, an “effective” second moment of inertia based on the gross moment of inertia I_g , and the cracked moment of inertia I_{cr} , is used to calculate deflections of an GFRP-reinforced beam. Due to the reduction of the moment of inertia in the cracked section, and consequently as for relaxation and greater deformation in the concrete, larger deflections occur.

M_{cr}/M_a ratio also determines the effective moment of inertia of the section based on Branson equation, (1968,1977), [1]. The deflection may be calculated using elastic theory equations for uncracked sections. If M_a increases over M_{cr} , cracks start to show up in the concrete section, starting from the supports, and later in the middle span, so the moment of inertia is suddenly decreased in the section from I_g to I_{cr} .

Between cracks, tension is transferred from the reinforcement to the concrete, by bond stresses (tension stiffening phenomenon), so Branson, proposed the use of the effective moment of inertia I_e :

$$I_e = \left(\frac{M_{cr}}{M_a}\right)^3 \cdot I_g + \left[1 - \left(\frac{M_{cr}}{M_a}\right)^3\right] \cdot I_{cr} \leq I_g \quad (1)$$

Where I_e - effective moment of inertia, M_{cr} - the moment in the section at the first cracking, I_g - gross moment of inertia, M_a - the maximum moment in the section where the deflection is calculated, I_{cr} - the cracked section moment of inertia [1].

The relationship between the acting moment and the moments of inertia are shown in Fig. 2.

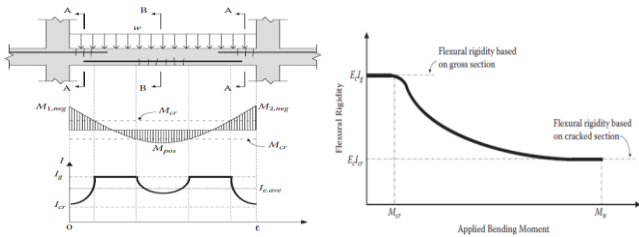


Fig. 2 Moment of inertia for a continuous beam and relationship between moments and moment of inertia

The "tension-stiffening" phenomenon affects the stiffness, deformations and cracks of the elements working in bending, so in Branson's equation, its effect depends on the ratio between the gross moment of inertia and that of the cracked section I_g/I_{cr} , and increases significantly if this ratio goes above 3. In beams reinforced with FRP bars, this ratio usually goes above 5, so Branson's equation underestimates the deformations of these beams.

Table 1: Comparison of main methods and design codes of the effective moment of inertia [13], [14].

Reference	Models for I_e
ACI 318 R -95 (1995) Branson's formula	$I_e = \left(\frac{M_{cr}}{M_a}\right)^3 \cdot I_g + \left[1 - \left(\frac{M_{cr}}{M_a}\right)^3\right] \cdot I_{cr} \leq I_g$
Benmokrane (1996)	$I_e = \frac{I_g}{7} \cdot \left(\frac{M_{cr}}{M_{max}}\right)^3 + 0.84 \cdot I_{cr} \cdot \left[1 - \left(\frac{M_{cr}}{M_{max}}\right)^3\right] \leq I_g$
ACI 440.1R -03 (2003)	$I_e = \frac{I_g}{\beta} \cdot \left(\frac{M_{cr}}{M_{max}}\right)^3 + \alpha \cdot I_{cr} \cdot \left[1 - \left(\frac{M_{cr}}{M_{max}}\right)^3\right] \leq I_g$ $\frac{1}{\beta} = \alpha' \cdot \left(\frac{E_{FRP}}{E_s} + 1\right) \leq 1, \alpha' = 0.5 \text{ and } \alpha = 1$
Yost (2003) based on ACI	$I_e = \left(\frac{M_{cr}}{M_a}\right)^3 \cdot \beta_d \cdot I_g + \left[1 - \left(\frac{M_{cr}}{M_a}\right)^3\right] \cdot I_{cr} \leq I_g$ $\beta_d = a_b \cdot \left(\frac{E_{FRP}}{E_s} + 1\right) + 0.13$ $a_b = 0.064 \cdot \left(\frac{\rho_{FRP}}{\rho_b}\right) + 0.13$
ACI 440.1R -06 (2006)	$I_e = \left(\frac{M_{cr}}{M_a}\right)^3 \cdot \beta_d \cdot I_g + \left[1 - \left(\frac{M_{cr}}{M_a}\right)^3\right] \cdot I_{cr} \leq I_g$ $\beta_d = \frac{1}{5} \cdot \left(\frac{\rho_{FRP}}{\rho_b}\right) \leq 1$
Rafi & Najjai (2009)	$I_e = \left(\frac{M_{cr}}{M_a}\right)^3 \cdot \beta_d \cdot I_g + \left[1 - \left(\frac{M_{cr}}{M_a}\right)^3\right] \cdot \frac{I_{cr}}{\gamma} \leq I_g$ $\gamma = \left(0.0017 \cdot \frac{\rho_{FRP}}{\rho_b} + 0.8541\right) \cdot \left(1 + \frac{E_{FRP}}{E_s}\right) \leq 1 \text{ or } \gamma = 0.86 \cdot \left(1 + \frac{E_f}{200}\right) \text{ in GPa}$ $\beta_d = \frac{1}{5} \cdot \left(\frac{\rho_{FRP}}{\rho_b}\right) \leq 1$
EC2-CEB, Italian Code CNR-DT 203/2006	$f = f_1 \cdot \beta_1 \cdot \beta_2 \cdot \left(\frac{M_{cr}}{M_{max}}\right)^m + f_2 \cdot \left[1 - \beta_1 \cdot \beta_2 \cdot \left(\frac{M_{cr}}{M_{max}}\right)^m\right]$ $m = 2$
Toutanji & Saafi (2000)	$I_e = \left(\frac{M_{cr}}{M_a}\right)^m \cdot I_g + \left[1 - \left(\frac{M_{cr}}{M_a}\right)^m\right] \cdot I_{cr} \leq I_g$ $m = 6 - \frac{10 \cdot E_f}{E_s} \cdot \rho_f$ if $\frac{E_f}{E_s} \cdot \rho_f < 0.3$ so $m = 5.98$ $m = 3$ if $\frac{E_f}{E_s} \cdot \rho_f \geq 0.3$
Alsayed Modeli A (2000)	$I_e = \left(\frac{M_{cr}}{M_a}\right)^m \cdot I_g + \left[1 - \left(\frac{M_{cr}}{M_a}\right)^m\right] \cdot I_{cr} \leq I_g$ $m = 5.5$
Alsayed Modeli B (2000)	$I_e = I_{cr}$ for $\frac{M_a}{M_{cr}} \geq 3$ $I_e = \left[1.4 - \frac{2}{15} \cdot \left(\frac{M_a}{M_{cr}}\right)\right] \cdot I_{cr}$ for $1 < \frac{M_a}{M_{cr}} < 3$
Bischoff (2005,2007) & Scanlon (2007)	$I_e = \frac{I_{cr} \cdot I_g}{1 - \left(1 - \frac{I_{cr}}{I_g}\right) \cdot \left(\frac{M_{cr}}{M_a}\right)^2}$
Abdalla based on ACI (2002)	$I_e = \frac{I_g \cdot I_{cr}}{I_{cr} \cdot \xi + 1.15 \cdot I_g \cdot (1 - \xi)}$ $\xi = \frac{0.5 M_{cr}}{M_a}$
Abdalla, Rizkalla & El Badry (EC2)	$f = \left(\frac{M_{cr}}{M_a}\right)^3 \cdot \beta \cdot f_1 + \left[1 - \beta \cdot \left(\frac{M_{cr}}{M_a}\right)^3\right] \cdot \alpha \cdot f_2$ $\alpha = 0.85 \text{ and } \beta = 0.5$

Deformations must be checked both for short-term and long-term loads, taking into consideration the phenomenon of fatigue. This methodology was adopted from ACI 318R-95 for calculating deformations for short-term acting loads. In these years, many researchers, based on experimental tests, proposed adjustments to Branson's equation, in order to have new approach in I_e calculations.

A summary of the main methods and design codes in calculating effective moments of inertia and deflections, without entering in details of their modifications of Branson's equation, are given in Table 1, [2], [3], [4], [5], [6], [7], [8], [9], [10], [11], [12], [16].

The deflections calculated both with the methods of the effective moment of inertia, as with the method of curvature (elastic line) of the beam, must fulfill certain conditions regarding permissible deformations in the concrete elements. It should be noted that if the deflections calculated using the moment of inertia of the cracked section satisfy the allowable values, then there is no need to use the effective moment of inertia.

4. Experimental testing of serviceability behavior of GFRP - RC beams

This paper contains experimental data derived from laboratory tests conducted on four reinforced concrete beams with GFRP bars. The purpose of these tests is the observation of deflections of the beams under the action of two concentrated loads. At the end, the results will be compared with theoretical calculations.

The cross-section of the beams is 250 X 400 mm, with 4000 mm span length, and 4200 mm total length. Because of the laboratory conditions and for not using concrete vibration, self-compacting concrete grade C30 was used. The concrete was produced with 25 mm maximum aggregate size, 0.35-0.37 water-to-cement ratio and 323 kg/m3 cement content [13], [14].

Table 2: Mechanical properties of GFRP bars

Diameter	Cross section	Weight	Modulus of elasticity	Tensile strength	Tensile strength
SI (mm)	A (mm ²)	W (g/ml)	GPa	MPa	%
15.87	197.9	181	46	620	1.42

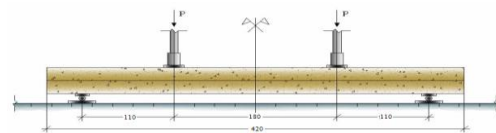


Fig. 3 Schematic view of the specimen



Fig. 4 The gaging system

Schematically, the beam specimens tested under four-points bending, are shown in Fig.5.

The tests would be carried out on four beams with different reinforcements. In the first pair of beams (beams T1 & T2), 4 Ø16 GFRP bars were used as longitudinal reinforcement, in the third beam (beam T3), 5 Ø16 GFRP bars, and in the fourth beam (beam T4), 2 Ø16 GFRP, while the upper reinforcement and staffs were not changed[13], [14].

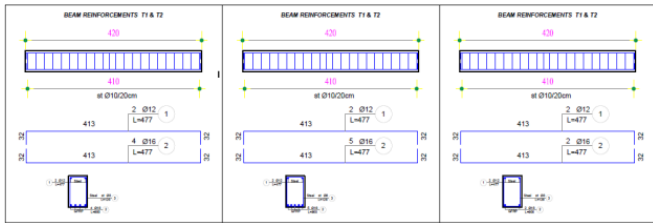


Fig. 5 The reinforcement of beams

Loading is done in cycles by scaling the electronic press at a loading rate of 300N/second. The first loading cycle was taken up to 10 kN, the second up to approximately 30 kN, the third cycle up to approximately 60 kN and the last cycle up to the failure of the beam. Only in T4 beam, this loading is done initially up to 10 kN, then up to 20 kN, up to 40 kN, and until the beam failure.



Fig. 6 Beam T1 & T2 - Concrete crushing failure, full cracked section (~90 kN)



Fig. 7 Beam T3 (~102 kN) & T4 (~55 kN) - Concrete crushing failure, full cracked section

5. Data analysis on deflection behavior

Experimental data are analyzed and are integrated in appropriate curvatures and are compared to theoretical calculations based on American Code ACI 440.1R -06.

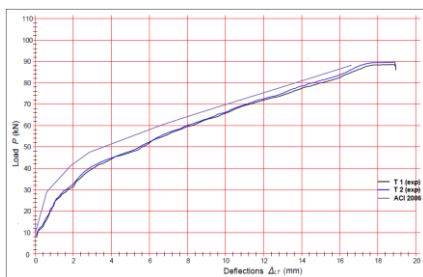


Fig. 8 Experimental vs predicted midspan deflection of T1 & T2

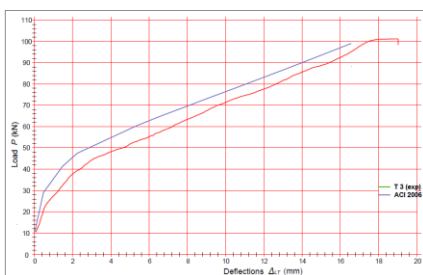


Fig. 9 Experimental vs predicted midspan deflection of T3

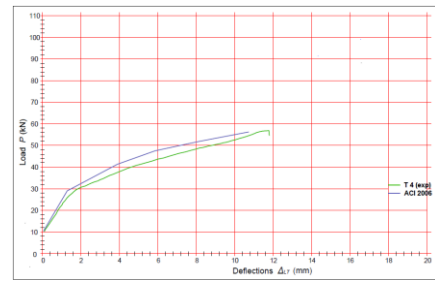


Fig. 10 Experimental vs predicted midspan deflection of T4

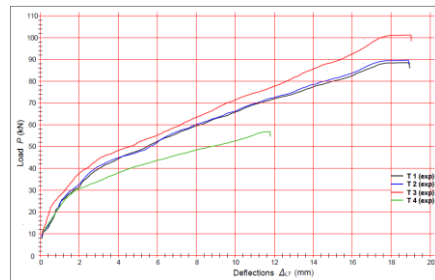


Fig. 11 Experimental midspan deflection of T1, T2, T3, T4.

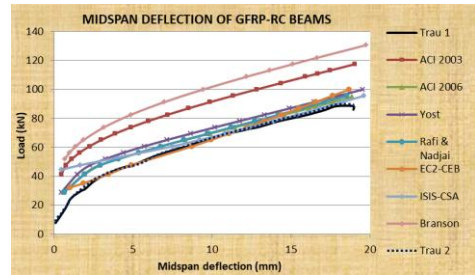


Fig. 12 Experimental vs theoretical midspan deflection of T1 & T2 for different design models

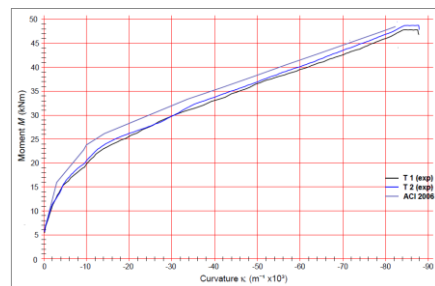


Fig. 13 Experimental vs predicted maximum curvature of T1 & T2

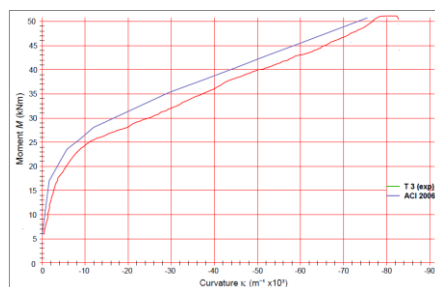


Fig. 14 Experimental vs predicted maximum curvature of T3

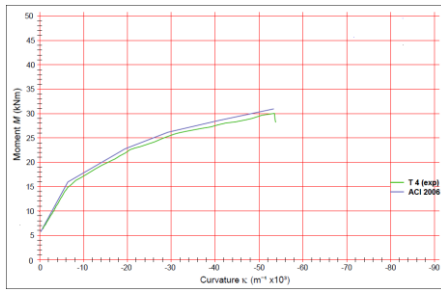


Fig. 15 Experimental vs predicted maximum curvature of T4

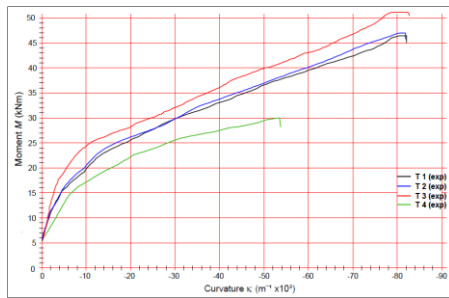


Fig. 16 Experimental maximum curvature of T1, T2, T3, T3

6. Test results and discussions

At the first pair of beams T1 & T2 (named TS1 & TS2 before test) were used 4 bars Ø16 GFRP, as longitudinal reinforcement with a theoretical balanced reinforcement ratio of $\rho_f = 0.00932 \approx \rho_{fb} = 0.0093$.

At beam T3 (named TS5 before test) were used 5 bars Ø16 GFRP, as longitudinal reinforcement, having a lightly overreinforced beam where $\rho_f = 0.0093 < \rho_f = 0.0116 < 1,4 \cdot \rho_{fb} = 0.0013$. At beam T3 (named TS5 before test) were used 2 bars Ø16 GFRP, as longitudinal reinforcement, having an underreinforced beam where $\rho_f = 0.00466 < \rho_{fb} = 0.0093$.

6.1 Results on deflection behavior

Figures 8, 9, 10, 11 and 12, show the experimental load-deflection response at midspan for all beams, compared to the theoretical calculations based on the American ACI 2006 code [14].

T3, is a slightly over-reinforced beam, so the concrete crushing occurs. The maximum deflection is slightly higher than in the case of T1 and T2, but still exceeds the allowable deflection before failure, corresponding to the ultimate load of 101.5 kN, which is about 14-15% higher than the ultimate load and for a reinforcement 25% greater than in the case of T1 and T2. The theoretical values are quite close to the experimental ones with a difference of only 5-6 kN (higher), or with a deflection of only 0.7-1mm smaller than the experimental values, so only 6-7% difference. This means that ACI 2006 gives expected good results for close to balanced and over-reinforced beams [14].

T4 is an under-reinforced beam, with half of the balanced reinforcement, that is, as much as 50% of the reinforcement of the beams T1 and T2, therefore the GFRP bars rupture occurs and after that, the concrete in the pressed area is crushed by the immediate deflection as seen in figure 16. It appears that this failure occurred for a much smaller load than in the case of T1 and T2, only 56.9 kN or 35-36% less. Also, the deflection at the failure moment is 11.8 mm, much less than the allowable deflections and also the deflections of beams T1 and T2. It can be seen that the predicted values are very close to the experimental ones with a difference of less than 3% [14].

Figure 17 shows the beam deflection–reinforcement ratio at rupture load of T4 for P = 56.9 kN. The greater the reinforcement, the smaller the deflections, and this go almost linearly in inverse proportion. ACI 2006 gives good results for under-reinforced or slightly over-reinforced beams, but it seems that the tendency is that error tends to increase almost proportionally with the beam reinforcement increment as shown in Figure 18, [14].

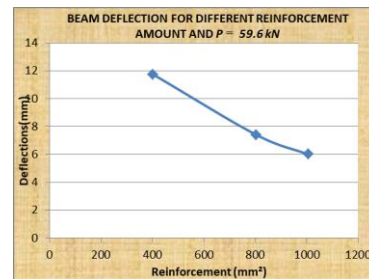


Fig. 17 Beam deflection – reinforcement ratio at rupture load of T4

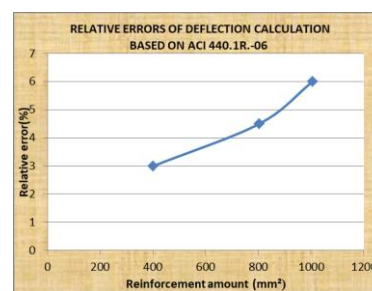


Fig. 18 Relative errors of deflection – reinforcement ratio based on ACI 440.1R-06

6.2 Results on curvature behavior

Figures 13, 14, 15, and 16 show the experimental load-curvature response at midspan for all beams, compared to the theoretical calculations based on the American ACI 2006 code.

We can see that the values obtained experimentally for T1 & T2 beams follow the same trend as deflections and are very close to each other with only a 2-3% difference. Also, the predicted values are quite close to the experimental ones with a difference of about 5%. The maximum bending moment in the section until the failure is 46.9 kNm for beam T1 and 47.8 kNm for beam T2, while the predicted ones are around 50.2 kNm. The maximum curvature value is about $90 \cdot 10^{-3} m^{-1}$ at T1 beam [14].

For beam T3 the maximum bending moment is 51.1 kNm while the predicted one is 54.7 kNm, with a difference of 7%. The maximum curvature is $82 \cdot 10^{-3} m^{-1}$, or about 8.5% less than for beams T1 and T2.

For beam T4 due to insufficient reinforcement and rupture of the GFRP bars, the maximum bending moment is only 30 kNm, and the predicted one is 31 kNm, having a difference of about 3%. The maximum curvature is $54 \cdot 10^{-3} m^{-1}$, around 40% smaller than for beams T1 and T2 [14].

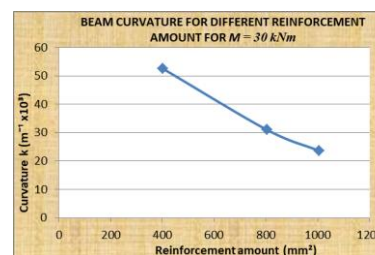


Fig. 19 Beam curvature – reinforcement ratio at rupture moment of T4

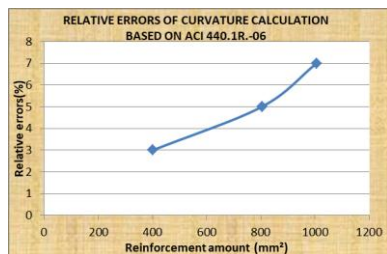


Fig. 20 Relative errors of curvature – reinforcement ratio based on ACI 440.1R.-06

Figure 19 shows the beam curvature – reinforcement ratio at rupture moment of T4 for $M = 30$ kNm, the greater the reinforcement, the smaller the curvature, and this goes almost linearly, in inverse proportion. ACI 2006 gives good results for under-reinforced or slightly over-reinforced beams, but it seems that the tendency is that the error tends to increase almost proportionally with the beam reinforcement increment as shown in Figure 20, slightly more pronounced than the one for the deflections [14].

7. Conclusions

After the experimental results analysis and their comparison with the theoretical predictions based on ACI 440.1R.-06, we can summarize the most relevant conclusions as follows:

1. The failure of GFRP reinforced concrete beams, when they have a balanced reinforcement ratio, or when they are slightly over-reinforced (around 40% more than the balanced one), occurs in a similar way as the failure of steel-reinforced beams, due to concrete crushing in the compression zone.

2. The failure of under-reinforced GFRP reinforced concrete beams, occurs in a different way from the failure of steel-reinforced beams, due to GFRP bar rupture in the tension zone, since the FRP reinforcement will not yield.

3. The prevailing problem of the tested beams seems to be cracking and deflections, and not the flexural capacity, except for the under-reinforced beam.

4. During the deflection and curvature analysis, is noted their trend increases with the decrease of the reinforcement ratio. The limit of theoretical prediction of deflections is achieved before the beam failure, except for the under-reinforced beam, when the failure occurs for rupture before having large deflections [14], [15], [17].

5. During the comparison between theoretical predictions based on ACI 440.1R.-06 and experimental results, was noted that this design code is quite accurate for calculating the deflections and beam curvature with slightly differences of 4-7% [14].

6. Also other methods and design codes such as Yost, Rafi & Nadjai, ISIS Canada, EC2 – CEB & Italian Code CNR, give good theoretical predictions regardless of the method used. The differences with experimental results are in the range of 3-8%, due to theoretical empiricism, and for not taking into account parameters that affect the effective moment of inertia I_e , such as: the reinforcement ratio ρ_f , the low FRP modulus of elasticity E_f , the initial deflections of the uncracked, the bond behavior of FRP bars with concrete, the loading type and tension-stiffening effect [14].

7. Is noted the trend to have bigger errors of the theoretical predictions, with the increase of reinforcement ratio, so their curvature is quite proportional.

Although the expectation based on theoretical predictions was appropriate (except for beam T4), these specimen tests were not enough to carry out important remarks for improving the design equations for calculating deflections and crack width of GFRP reinforced concrete beams and are needed for other research.

8. References

- [1] Branson, D.E., Deformation of Concrete Structures, New York: McGraw-Hill, 1977.
- [2] Abdul Rahman MS., Narayan SR. "Flexural behaviour of concrete beams reinforced with glass fiber reinforced polymer bars." J Kejuruteraan Awam 2005;17(1):49–57.
- [3] ACI Committee 440. ACI 440.1R-06, Guide for the design and construction of concrete reinforced with FRP bars." Farmington Hills, Mich., USA: American Concrete Institute (ACI); 2006.
- [4] Al-Sunna Raed., Pilakoutas K., Hajirasouliha I., Guadagnini M., "Deflection behavior of FRP reinforced concrete beams and slabs: an experimental investigation." Compos Part B Eng 2012;43(5):2125–34 [Online publication: 1-Jul-2012].
- [5] Barris, P. C., Llinas, Ll. T., "Serviceability behavior of fibre reinforced polymer reinforced concrete beams" [Ph.D. thesis]. Girona, Catalonia, Spain: University of Girona; 2010.
- [6] Benmokrane, B., Chaallal, O., Masmoudi, R., (1996a), "Flexural response of concrete beams reinforced with FRP reinforcing bars", ACI Structural Journal, Vol. 93, No. 1, pp. 46–55.
- [7] Bischoff, P., Scanlon, A., "Effective moment of inertia for calculating deflections of concrete members containing steel reinforcement and FRP reinforcement". ACI Struct J 2007;104(1):68–75.
- [8] CAN, CSA S806-02. "Design and construction of building components with fibre-reinforced polymers". Rexdale, Ontario, Canada: Canadian Standards Association; 2002. 177 pp
- [9] CEB-FIB Bulletin, "FRP reinforcement for RC structures", 2006.
- [10] Yost, J., Gross, S., Dinehart, D., "Effective moment of inertia for glass fiber-reinforced polymer-reinforced concrete beams". ACI Struct J 2003; 100(6):732–9.
- [11] El-Nemr, A., Ahmed, A. E., Benmokrane B., "Flexural behavior and serviceability of normal and high-strength concrete beams reinforced with glass fiber-reinforced polymer bars". ACI Struct J 2013;110(6).
- [12] Fatih, K. I., Ashraf, A. F., "Flexural performance of FRP reinforced concrete beams". J Comp Struct 2012;29 [Available Online 29 December 2011].
- [13] Deneko, E., Gjini, A. F., "The Influence of the Effective Moment of Inertia on the Deflection of FRP Reinforced Concrete Members". European Academic Research Vol.III, Issue 4/ July 2015 ISSN 2286-4822
- [14] Deneko, E. "Use of FRP bars as internal reinforcement in concrete members.", Doctorate thesis in Civil Engineering, Polytechnic University of Tirana, 2017.
- [15] Faza, S. S., and Ganga Rao, H. V. S.,(1993), "Theoretical and experimental correlation of behavior of concrete beams reinforced with fiber reinforced plastic rebars, in Fiber-Reinforced-Plastic Reinforcement for Concrete Structures", SP-138, American Concrete Institute, Farmington Hills, MI, pp. 599–614.
- [16] Mousavi, R. S., Reza, E. M., "Effective moment of inertia prediction of FRP-reinforced concrete beams based on experimental results". ASCE J Comp Constr 2012;16 (5):490–8.
- [17] Nanni, A. (1993a), "Flexural behavior and design of reinforced concrete using FRP rods", Journal of Structural Engineering, Vol. 119, No. 11, pp. 3344–3359.